Cutter wear mechanisms in hard rock tunnel boring

Francisco Javier Macias[1,2]*, Jarand Nærland[3], Nuria Espallargas[3]

[1] JMConsulting-Rock Engineering AS, Trondheim, Norway

[2] NTNU, Faculty of Engineering Science and Technology, Dept. of Civil and Transport Engineering, N-7491 Trondheim, Norway.

[3]NTNU, Faculty of Engineering, Department of Mechanical and Industrial Engineering, Tribology Lab, Richard Birkelands vei 2B, 7491, Trondheim, Norway

Abstract

Cutter consumption and parameters such as cutter ring wear has a great relevance in the final excavation time and cost in hard rock tunnel boring machines (TBMs), especially in hard rock conditions. Cutter wear involves a complex tribological system that interacts also with the geologicy of the rock mass. Understanding the processes and failure mechanisms during cutter wear (e.g. modes of contact, wear, load effects) and assessing the influence of temperature on cutter ring wear processes enables new knowledge to be applied to get better cutter consumption predictions and future improvements in cutter ring development. In addition, it might be used to evaluate the suitability of the new rock abrasivity test method (Rolling Indentation Abrasion Test, RIAT) for assessing cutter ring wear.

Keywords: Hard rock tunnel boring, cutter wear, tribology, failure mechanism

1 Introduction

The hard rock Tunnel Boring Machine (TBM) method has become widely and generally used for underground development. TBM tunnelling performance and costs may be strongly influenced by the level of consumption of cutter discs, especially in hard and abrasive rock conditions. Cutter technology has experienced continuous development resulting in reliable cutters that are in use today (Roby et al., 2009). Thus, in order to achieve reliable planning and risk control, reliable methods for predicting cutter consumption are needed.

Limitations resulting from the quality of cutter ring steel are yet to be overcome nowadays. Current cutter ring steel technology does not permit the use of the full thrust capacity of current machines, but limits the long-term average cutter thrust per cutter for a 483 or 508 mm cutter diameter to 312 kN. A new generation of cutter material, allowing a higher thrust in hard rock conditions will increase TBM penetration rates and cutter life. In addition, improvements in cutter ring capacity will require corresponding improvements in rolling bearing capacity. An increase of 15% in the thrust applied may result in as much as a 50% increase in penetration. This in turn may reduce excavation costs and thus extend the scope of application of the TBM method (Bruland, 2000).

Many factors influence the number of cutters consumed during a hard rock TBM tunnelling project. Indeed, cutter discs consumption is an important parameter for tunnelling costs by TBMs. Abrasive wear has been confirmed to be the major factor during normal operations (Rostami, 1997; Bruland, 2000; Frenzel et al., 2008), combined with the influence of rolling distance.

The interaction between cutter rings and the rock mass during hard rock tunnelling entails a complex tribological system, and cutter ring wear is influenced by several different rock properties and machine parameters. Understanding the processes and failure mechanisms during cutter wear enables new knowledge to be applied to better cutter consumption predictions and future improvements in cutter ring development. The cutters are continuously worn out as boring takes place and are greatly influenced by many geological parameters, such as the rock drillability, abrasive minerals content, rock mass fracturing…Few realistic lab scale tests are available to experimentally simulate that complex interaction, therefore a new rock abrasivity test method named Rolling Indentation Abrasion Test (RIAT) has recently been developed (Macias et al., 2015; Macias et al, 2016; Macias, 2016). The RIAT method consists of miniature rolling discs penetrating the surface of an intact rock sample. The rotation, torque and vertical thrust of the tool are provided through a suitable drive unit.

In the present work, a comprehensive set of comparative analyses of worn cutter ring samples from three recently finalised TBM projects, and mini-cutter rings from the Rolling Indentation Abrasion Testing (RIAT) on standard rock samples has been carried out. The analyses have involved identifying TBM cutter ring failure mechanisms arising from tunnel boring and assessing the influence of temperature on cutter ring wear processes with the main objective of getting a better understanding of cutter wear processes and failure mechanisms to help life prediction accuracy.

2 Experimental methodology

2.1 Samples

Worn TBM cutter ring samples from actual TBM projects and worn mini-cutter rings from RIAT tests will be investigated. For further details concerning the RIAT test procedure, the reader is referred to Macias et al. (2016). The cutter discs in the actual TBM project were replaced due to excessive wear, and the samples taken had an initial diameter of 483 mm. Data regarding their position on the cutterhead, instantaneous cutter life and rock mass properties were obtained. The RIAT mini-cutter discs used in the tests are 30 mm in diameter with tip widths of 4 mm. The RIAT tests are performed on an intact rock sample. One of the TBM samples was subjected to a heat treatment (i.e. tempering) in order to find out the temperatures reached during operation. In section 2.4 details of this treament can be found.

Table 1 provides an overview of the analyses and tests performed on the TBM cutter discs and RIAT mini-cutter ring samples respectively.

Table 1. Overview of the cutter disc wear analysis tests. The symbol "◯" indicates that a test has been performed, while the symbol "-" indicates that the test has not been performed.

Sample ID	Sample type	Rock Type	Chemical composition	Hardness	Microstructure	FIB* cross sections	Tempering
01	TBM cutter	Gneiss	-	◯	◯	◯	-
02	TBM cutter	Gneiss	-	◯	◯	◯	-
03	TBM cutter	Gneiss	-	◯	◯	◯	-
04	TBM cutter	Gneiss	-	◯	◯	◯	-
05	TBM cutter	New	◯	◯	◯	-	◯
06, 07	RIAT cutter	Basalt	-	-	◯	◯	-
08, 09	RIAT cutter	Granite	-	-	◯	◯	-
10, 11, 12, 13	RIAT cutter	Granite	-	◯	◯	◯	-
14, 15, 16	RIAT cutter	Quartzite	-	-	◯	◯	-

*FIB = Focused Ion Beam

Figure 1 shows the worn TBM cutter ring and RIAT mini-cutter ring samples analysed in this paper.

Figure 1. Cutter ring sample 02 (left) and Mini-cutter ring samples (right).

2.2 Hardness measurements

Macro-hardness measurements were carried out on TBM cutter ring samples and micro-hardness measurements on RIAT tested mini-cutter ring samples.

A Matsuzawa Seiki-DVK-1S hardness indenter was used to perform the macro-hardness measurements. All measurements were carried out at 5 kgf, with the results expressed in HV5. Digital positioning of the optical microscope stage was used to measure the distance from the edge of the sample surface to the indentations, made along parallel lines extending from the edge of each sample. Three lines of indentations were measured for each sample in order to obtain an average (Figure 2).

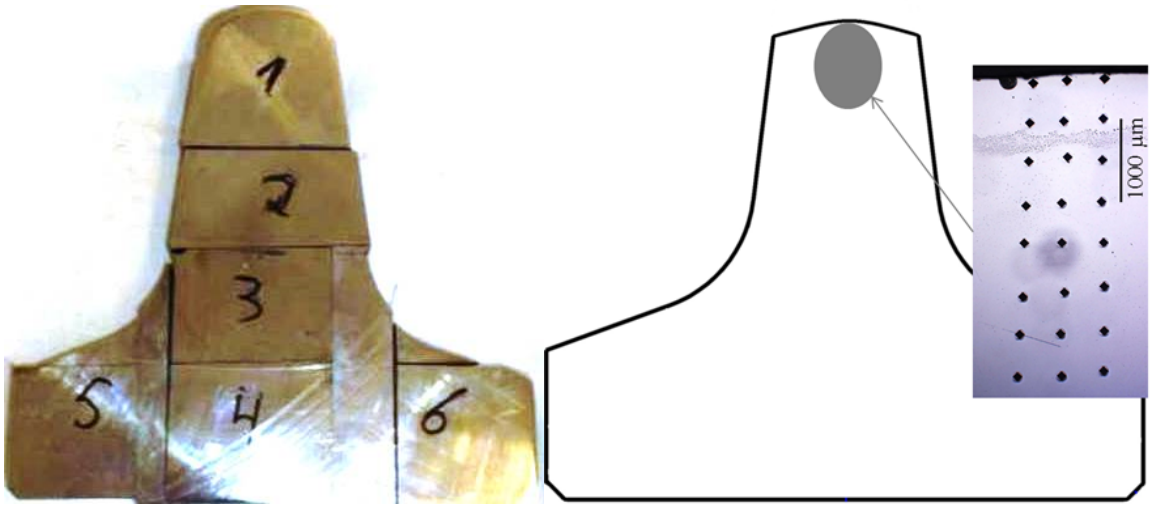

Figure 2. Image showing hardness indentations on a TBM cutter ring sample.

In the case of the hardness measurements made after the heat treatment (tempering), each sample was given ten indents, and an average value obtained. In this case, a Leica VMHT MOT micro-hardness indenter was used to measure the hardness profiles of RIAT mini-cutter samples. The process was similar to that described above except for the distance from indentation to surface. This was carried out manually by moving the sample stage by a pre-defined distance for each measurement. The measurements were performed at 0.025 kgf, with the results expressed in HV0.025.

2.3 Microstructure

Intial cutting of the sample slices from the cutter ring was performed using a large bandsaw with a tungsten carbide (WC) grid blade. The saw was water-cooled to keep temperatures below 25°C. The slices were subsequently cut into smaller samples using a water-cooled Discotom-2 saw fitted with a Struers 60A25 circular blade.

The samples were then embedded in a two-component epoxy mixture "Epofix^{TM}" in a cylindrical mould for microscopic examination. These samples were 30 mm in diameter and 15 mm thick. The circular surface of each cylindrical sample was ground with SiC paper and polished with a diamond suspension until a final roughness of less than 0.1 µm was achieved.

Sample preparation for optical microscopy also required an etching process in order to reveal the microstructure of the metallic samples. In the present work, the Marble's etchant reagent with a lower $CuSO_4$ concentration than in original compositions was used to avoid overetching (Table 2).

Table 2. Marble's metallographic etchant used for optical imaging (Nærland, 2015).

Composition	Effect
5 g $CuSO_4$ 50 ml HCl 50 ml water	Martensite turns dark. Ferrite, retained austenite and carbides unaffected.

A Leica MEF4M optical microscope was used to obtain microstructure images of 200X, 500X and 1000X magnification. A Zeiss Ultra 55 Limited Edition scanning electron microscope (SEM) was used to obtain surface images at higher magnifications. Secondary electrons were used for surface imaging. Heavier atoms reflect more electrons than lighter ones, and thus appear as bright areas on the image. All samples were cut and cleaned, followed by five minutes ultrasonic bath in acetone to remove dust, organic material and embedded rock debris from their surfaces. Some rock still remained on the surface and thus gold sputtering was performed to enhance conductivity and reduce image drift.

Focused Ion Beam (FIB) was used to cut cross sections of the samples without exposure to the air since the microscope enables standard SEM imaging and FIB simultaneously. A FEI Helios NanoLab DualBeam FIB microscope with a gallium sputtering source was used.

2.4 Tempering

Tempering was performed to identify the evolution of hardness as a function of time and temperature without inducing mechanical deformation. The samples were cut from an unused TBM disc. Tempering is a heat treatment process applied to hardened steels to increase ductility, as well as to relieve quenching stresses to ensure dimensional stability. The treatment requires heating the steel to temperatures between 250 and 650°C, depending on the properties required (Callister and Rethwisch, 2009). In the steels used for producing the cutter discs, retained austenite was found (see section 4.2). Therefore, tempering is used to transform the austenite into tempered martensite. Retained austenite is undesirable because it can later transform under stress to martensite. The volume expansion associated with transformation from austenite to martensite can initiate brittle fracture (Smading, 2016).

In this study, tempering was performed at 200, 300, 400, 500, 600 and 700°C. The hardness and microstructure of the tempered samples was analysed after the heat treatment and were compared to used cutter discs. Three samples were tested at each tempering temperature, using tempering periods of 1, 2 and 4 hours respectively. A Nabertherm N17 furnace was used for the tests (Nærland, 2015). No attempts were made to control the atmosphere inside the furnace. This will result in decarburization due to the presence of a lower carbon concentration in the air than in the steel. This phenomenon is consistent with normal TBM operations (during boring) and is therefore seen as a natural part of the experiment. Each sample was naturally cooled in air prior to examination.

3 Test results and discussion

3.1 Steel composition and microstructure

Table 3 provides an overview of the tests perfomed, and the characteristics of the cutter ring samples respectively. Table 3 shows the composition of the TBM cutter and RIAT mini-cutter rings. The values were measured by XRF for the TBM cutter disc and were provided by the supplier of the RIAT mini-cutter disc. The theoretical composition of a AISI type H13 tool steel in shown in Table 3 for refernce since it is typically used for TBM cutter rings with slightly modified values.

Table 3. Composition of the TBM cutter disc and RIAT mini-cutter samples.

Composition (wt. %)	TBM cutter disc*	RIAT mini-cutter disc**	AISI Type H13***
C	0.57	0.39	0.32 – 0.40
Mn	0.29	0.40	-
Si	0.98	1.00	1.00
Cr	4.84	5.20	5.13 – 5.25
V	0.92	0.90	1.00
Mo	1.35	1.40	1.33 – 1.40
Ni	0.12	-	-
Cu	0.12	-	-

*Average composition of a typical TBM cutter ring (Krogstad, 2013)
**Original composition (Uddeholm, 2015)
***AISI 2015

Figure 3 shows the optical microstructure of a cutter disc steel after methalographic preparation. The image shows a typical tempered martensite microstructure with some paler areas of retained austenite. The steel has been die-forged and heat-treated to increase its hardness (Espallargas et al, 2015).

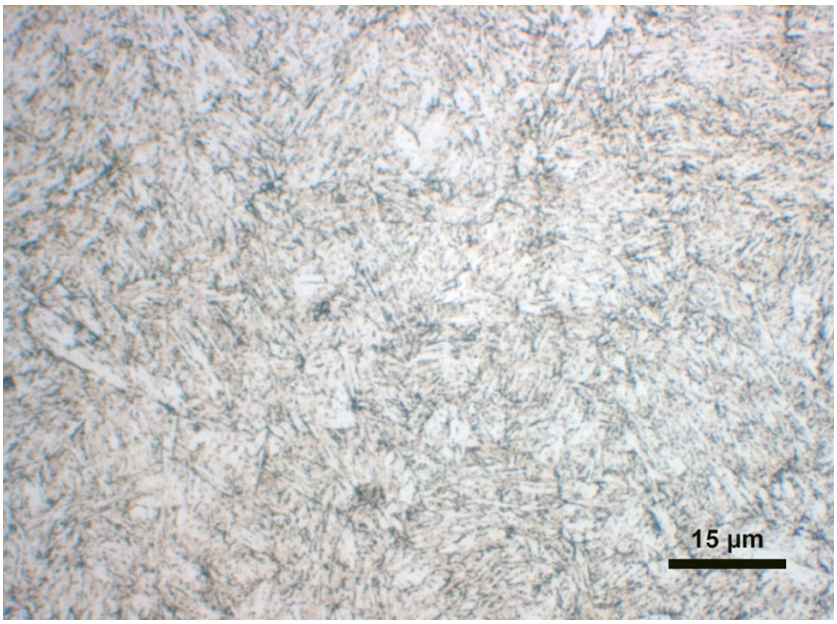

Figure 3. Microstructure of the cutter disc steel tested as part of this study.

3.2 Hardness

Macro and micro hardness measurements were performed on both the TBM cutter and RIAT mini-cutter rings on cross-sections parallel to the rolling direction. Some of the results from the TBM cutter and RIAT mini-cutter rings indicate work hardening due to an increase in hardness (about 10%) close to the cutter surface as shown in Figure 4 (right). However, in some other sample cross-sections, hardness decreases close to the surface indicating some degree of surface softening (Figure 4 left). As a general trend, a sharper gradient is observed for the RIAT mini-cutter samples than for the TBM samples.

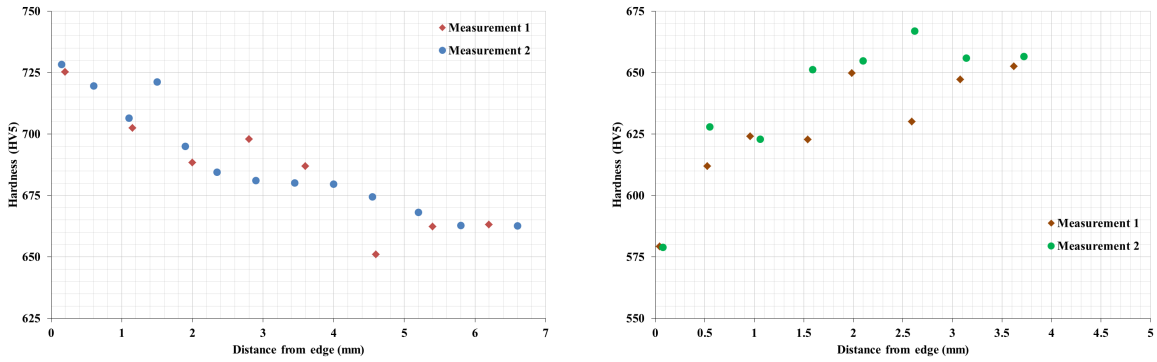

Figure 4. Hardness profiles for TBM cutter ring sample 02 (left) and sample 04 (right).

3.3 Influence of temperature on cutter wear

Hardness was studied as a function of time and temperature after tempering. It is commonly assumed that the representative boring time for one stroke (approx. 1.8 m) for hard rock tunnel is 1 hour. Therefore the minimum tempering time chosen in the experiments was 1 hour. Interestingly, the hardness results for different tempering times (1, 2 and 4 hours) exhibited similar trends. Therefore in Figure 5 only the results for the test performed at 1 hour are shown. The hardness decreases from approximately 670 HV5 at 500°C to 300 HV5 at 700°C.

If the surface hardness of a cutter disc is known, Figure 5 can be used as a master curve for finding the temperature at which a disc (of the same composition as the one tempered) has been subjected. Plotting the hardness of the TBM cutter disc sample 04 from Figure 4 on Figure 5, it is found that the temperature required to obtain the surface hardness value measured after failure (Figure 4) is in the range of 620°C. On the other hand, for TBM cutter disc sample 02 a temperature in the range of 450°C is required to obtain the surface hardness value measured after failure (Figure 4). These results indicate that for a cutter disc to suffer softening (sample 04) a higher temperature is required.

However, there is also an effect of the depth. The results in Figure 5 indicate a clear temperature gradient that decreases with depth below the worn surface of the sample. By plotting the measured hardness at a known wear depth into the cutter surface (2 and 3 mm for

sample 04), temperatures of 540 and 320°C can be predicted/expected for each depth respectively.

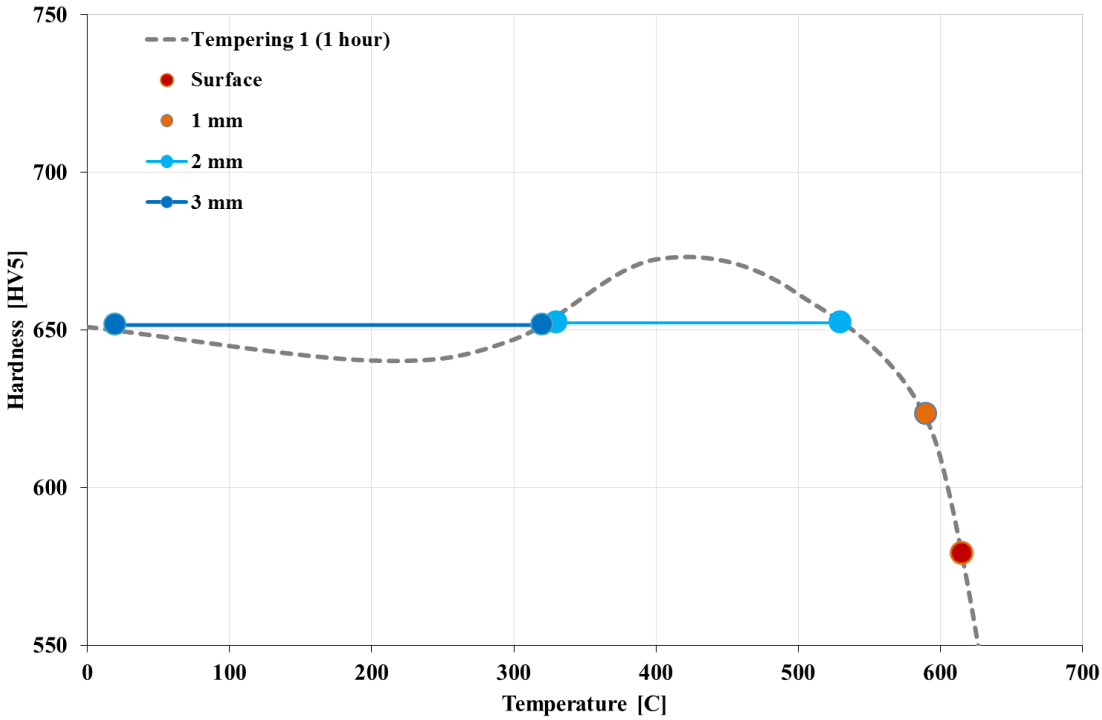

Figure 5. Hardness profile resulting from a tempering experiment performed for 1 hour on TBM cutter ring sample no. 04. Points and horizontal lines indicate hardness values at known distances from the wear surface of the sample.

3.4 Failure mechanism

3.4.1 Modes of contact

Analysis of cross-sections parallel to the direction of rolling was carried out to find the mode of contact. Lamellar structures at the surface with signs of plastic deformation, running parallel to the rolling direction, may be caused by a sliding contact mode and the depth of this layer might indicate the dominance of sliding versus rolling (Nærland, 2015). None of the TBM cutter rings showed signs of sliding contact instead, cracks running parallel to the surface are found (Figure 6). This indicates that rolling behaviour is the dominant mechanism, beyond of geological factors.

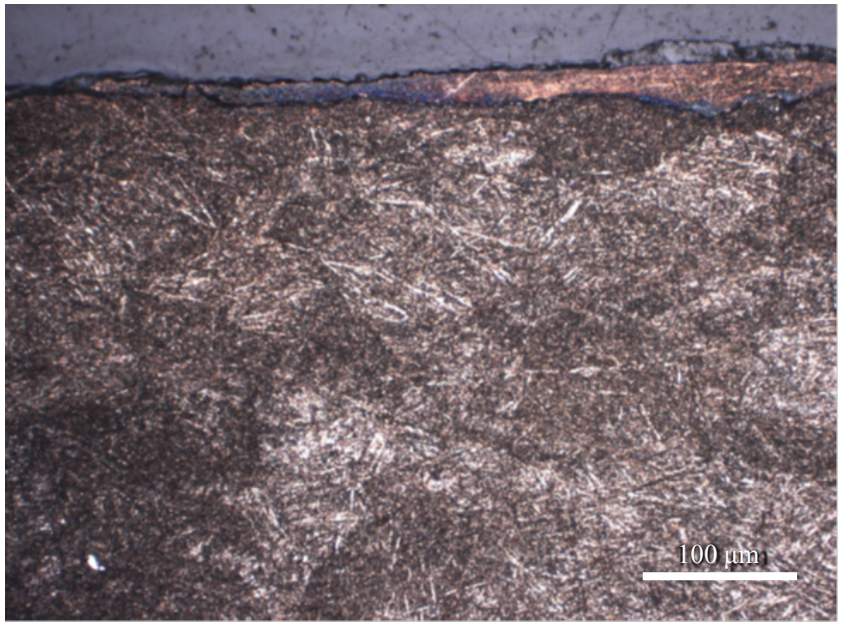

Figure 6. An optical image of a cross-section cut parallel to the rolling direction of a TBM cutter ring (sample 03). Reproduced from Nærland (2015).

On the other hand, the results from analyses of the RIAT mini-cutter ring samples revealed lamellar structures with severe plastic deformation when testing aginst quartzite, granite and basalt (Figure 7). The presence of these layers indicates a greater contribution of sliding to the contact mode in the case of RIAT tests, which at the same time might indicate the use of excessive thrust during testing.

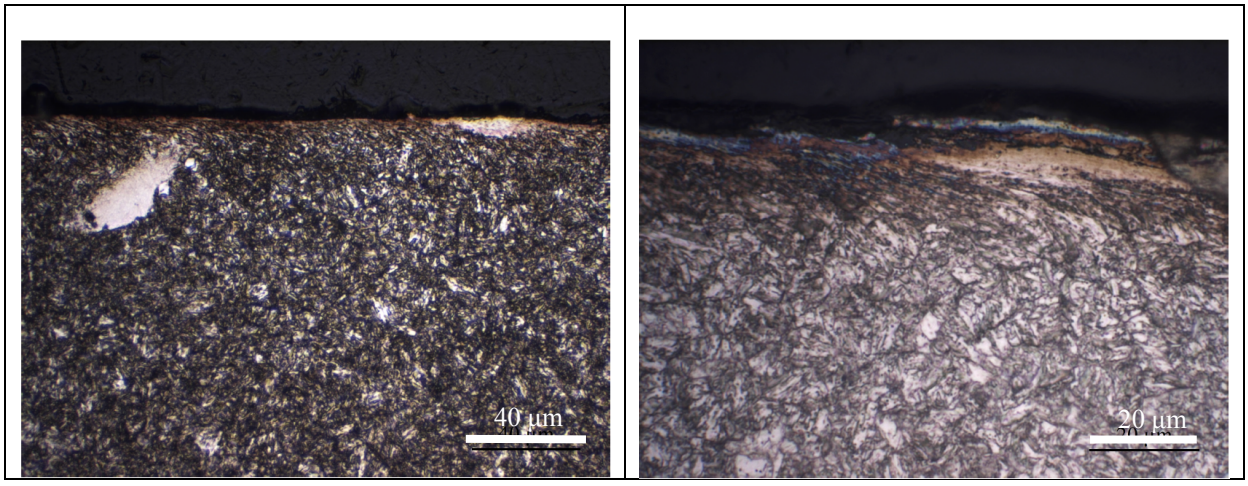

Figure 7. Optical images of cross-sections cut parallel to the rolling direction of RIAT mini-cutter ring sample 15 (left) and 11 (right). Reproduced from Nærland (2015).

The lamellar layer was observed to vary in thickness with values that correlated with rock abrasiveness. The largest thickness value was found for tests using granite (sample 11) and the lowest for quartzite (sample 15). The lower the abrasivity, the greater the thickness of the lamellar layer. This correlation is in good agreement with the research findings of Petrical et al. (2014) for martensitic steels under two-body abrasion conditions.

A different mode of contact in TBM versus RIAT tests will probably imply different wear mechanisms. Less plastic deformation in the case of the rolling contact (TBM) is seen and therefore more brittle fracture (i.e. chipping) due to fatigue should be expected. Whereas in the case of the RIAT, the plastic deformation resulting from the sliding contact will result in a mushrooming type of wear and more abrasion.

3.4.2 Wear mechanisms

The optical microscope images presented in Figure 8 make it possible to distinguish fatigue in the cross sections both parallel and perpendicualr to the rolling direction. This is evidenced by the presence of cracks running parallel to the surface. The formation of such cracks indicates fatigue initially originated by the rolling contact mode. Cracks connected to the surface may have a subsurface origin, or may result from the folding of asperites by plastic deformation leading to crack growth caused by fatigue. Interestingly, no severe plastic deformation is observed in these cross sections, as expected from a fatigue type of wear.

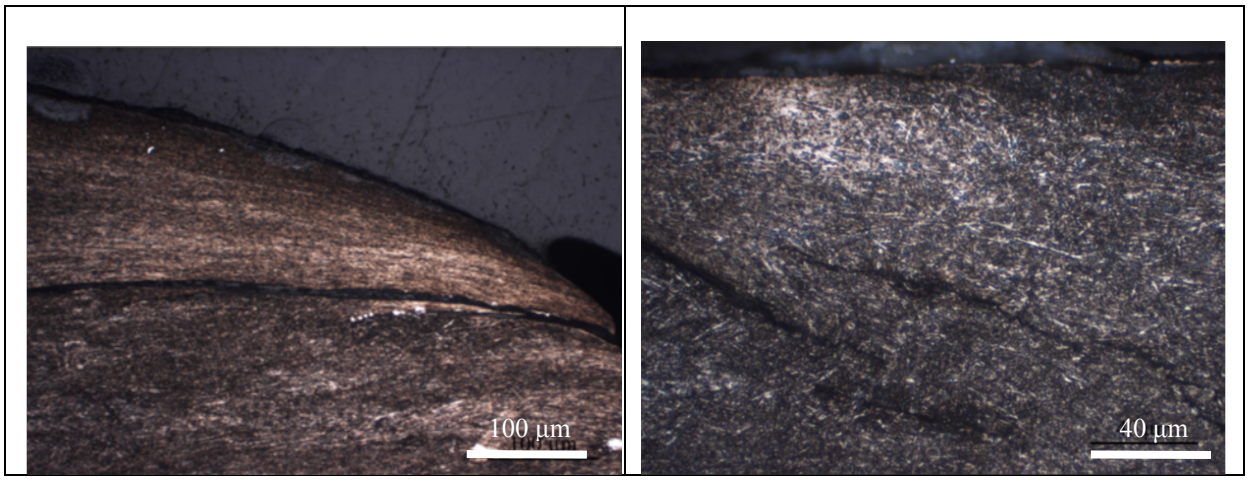

Figure 8. Optical images of cross-sections taken from TBM cutter ring sample 02. The cross-sections are cut perpendicular (left) and parallel (right) to the rolling orientation. Reproduced from Nærland (2015).

As previously discussed, subsurface cracks are clear indications of wear caused by fatigue, which is a common result of rolling contacts. The mechanism called “chipping”, which is commonly cited as a reason to replace TBM cutters under hard rock conditions, arises when subsurface cracks reach the surface of the cutter producing a chip of material that detaches from the steel. Figure 8 (right) provides an example of visible cracks initiated in the subsurface clearly indicating fatigue. These cracks, when reaching the surface after repeated cycles, will release debris by way of chipping.

On the other hand, the wear mechanisms observed for the RIAT samples are more related to abrasion and folding of asperities by plastic deformation (Figure 9 left and center). From the tests performed, it is reasonable to assume that fatigue would make a greater contribution to wear if the tests were run for longer periods and lower thrust increasing the rolling

contribution to the contact mode. The abrasive wear on the surface of the cutter discs was analysed using an electron microscope, and it is clear by the lines produced by abrasive ploughing (Figure 9 right). The bright areas of that image indicate the presence of embedded rock debris (Nærland, 2015). The most pronouned wear lines were identified in RIAT mini-cutter ring samples tested using quartzite. This is to be expected since quartzite is the most abrasive rock type. The higher the abrasion type of wear, the lower the plastic deformation. This is clearly seen in the more pronounced folding of the sample tested against basalt (Figure 9 right) with respect to the one tested aginst granite (Figure 9 center).

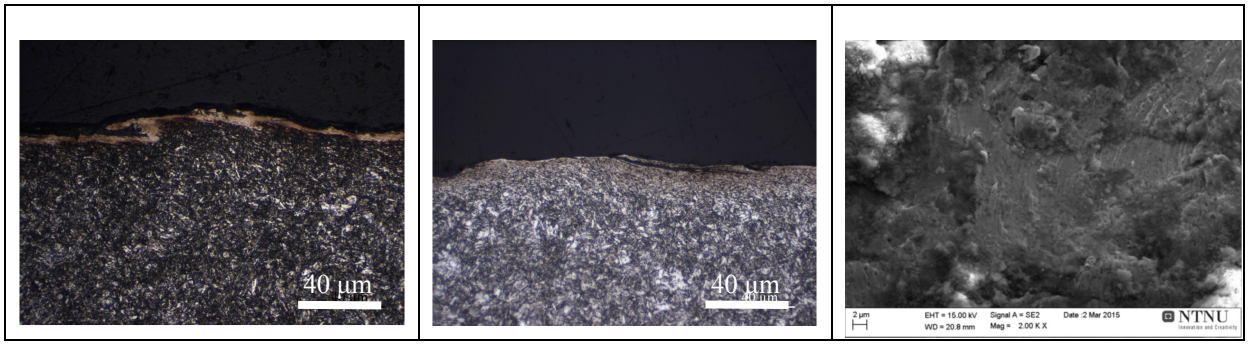

Figure 9. Folding due to plastic deformation in RIAT cutter 07 (left) and cutter 11 (center). SEM surface image of RIAT cutter 15 (right). Reproduced from Nærland (2015).

3.4.3 Load effect

Figure 10 and 11 show FIB cross-sections from TBM cutter ring and RIAT samples illustrating the presence of a martensitic microstructure and interestingly revealing carbides (seen as black dots and identified as mostly vanadium carbide) (Nærland, 2015). Figure 10 (left) shows no evidence of nanocrystalline grain structures for TBM cutter ring sample 01 confirming the low contribution of plastic deformation to the fatigue wear. Instead grooves on the surface are observed depicting the chipping wear mechanism. Interestingly, a thin nano-crystalline layer (above the dashed line) indicating some contribution of sliding wear has been observed in areas of the TBM cutter samples where no chipping was found (Figure 10 right). However the plastic deformation observed is smaller than the one observed in the RIAT samples (Figure 11).

Both the RIAT mini-cutter ring sample 07, which was tested using basalt, and sample 15, tested using quartzite show similar patterns to the TBM cutter ring samples (Figure 11). The RIAT mini-cutter ring worn by basalt shows a thicker deformation layer than the sample worn by quartzite. A more abrasive rock will generate less plastic deformation due to the lower contribuion of the sliding mode of contact as already mentioned earlier.

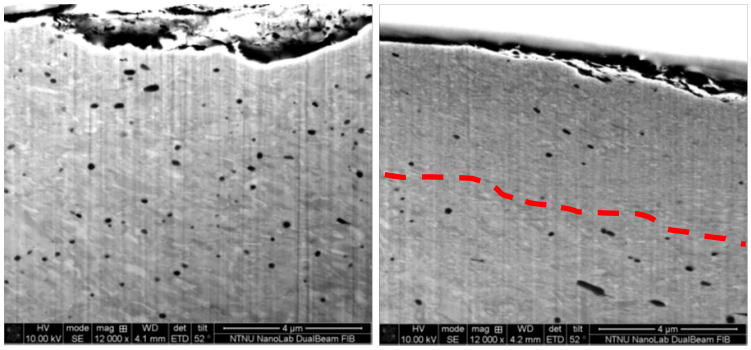

Figure 10. A FIB image of a cross-section (perpendicular to rolling direction) from TBM cutter ring sample 01 (left) and sample 04 (right). Above the dash line nano-crystalline layer is found. Reproduced from Nærland (2015).

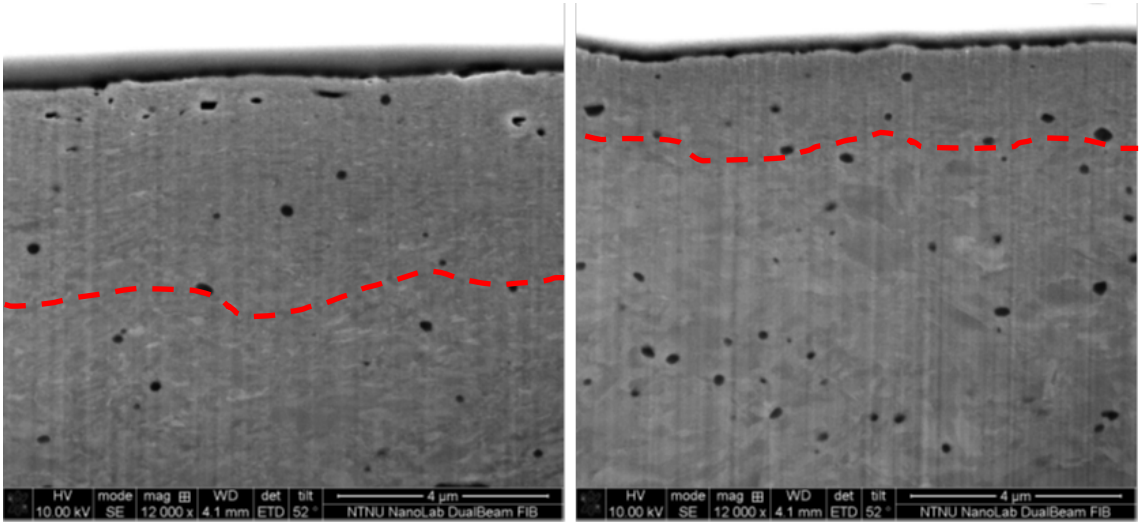

Figure 11. FIB images of cross-sections (perpendicular to the rolling direction) from RIAT mini-cutter ring sample 07 (left) and 15 (right). Above the dash line nano-crystalline layer is found. Reproduced from Nærland (2015).

4 Conclusions

The main objective of this research was to get a better understanding of cutter wear processes and failure mechanisms and therefore improve cutter life prediction accuracy. This work might be useful for cutter technology and development of the new rock abrasivity test method (RIAT). Following, the conclusive remarks are listed:

1. An increase in chipping of cutters is observed to correlate with reduced rock abrasivity and increased fatigue type of wear in the cutters. This can be explained by prolonged exposure to cyclic loads and higher load peaks during boring.
2. Abrasive wear has been demonstrated to occur in the TBM cutter ring and RIAT mini-cutter ring samples. Rolling is indicated as the primary mode of contact in the case of the TBM cutter ring samples, but represents a less dominant component for the RIAT mini-cutter ring samples. This can be explained by the restricted rolling diameters applied during laboratory scale testing.

3. Cracks have been identified in the subsurface steel of TBM cutters, and are interpreted to have been produced by fatigue.
4. Test results indicate the presence of work hardening in TBM cutter samples and RIAT mini-cutter rings. The amount of hardening is similar for both, with an increase in hardness of approximately 10%.
5. Some of the TBM cutter rings exhibited the presence of softening which may be the result of high temperatures induced during boring. The tempering tests indicate that a maximum temperature of 620°C was achieved in the surface layer of several TBM cutter ring samples. Temperatures of between 540 and 320°C are found at 2 and 3 mm depths from the cutter surface respectively. This temeprature dependency might play an important role in cutter ring wear.

Acknowledgements

The authors would like to thank the research project "Future Advanced Steel Technology for Tunnelling" (FAST-Tunn). This project was managed by SINTEF/NTNU, and funded by the Research Council of Norway. The Robbins Company, BASF Construction Chemicals, the Norwegian Railroad Authorities, Scana Steel Stavanger, BMS steel, the LNS Group and Babendererde Engineers were industrial and funding partners of the project.

References

AISI Type H13 Hot Work Steel, Mat Web. Available online at http://www.matweb.com/search/datasheet_print.aspx?matguid=e30d1d1038164808a85cf7ba6aa87ef7

Bruland, A. (2000). Hard Rock Tunnel Boring: Vol. 1-10. PhD thesis, Norwegian University of Science and Technology (NTNU), Trondheim, Norway.

Espallargas, N., Jakobsen, P.D., Langmaack, L. and Macias, F.J. (2015). Influence of corrosion on the abrasion of cutter steels used in TBM tunnelling. Rock Mechanics and Rock Engineering, Vol 48 (2015), pp 261–275.

Frenzel, C., Käsling, H. and Thuro, K. (2008). Factors influencing Disc Cutter Wear. Geomechanics and Tunnelling Vol 6 (2008), pp 55-60.

Macias, F.J., Dahl, F.E. and Bruland, A. (2015). New rock abrasivity test method by rolling disc. Proceedings of the 13th Congress on Rock Mechanics, ISRM Congress 2015 - In-novation in Applied and Theoretical Rock Mechanics, May 10-13, 2015, Palais des Congrès der Montréal, Canada, Paper 634, 10 p., ISBN: 978-1-926872-25-4 634.

Macias, F.J., Dahl, F.E. and Bruland, A. (2016). New rock abrasivity test method for tool life assessments on hard rock tunnel boring: The Rolling Indentation Abrasion Test (RIAT). Rock Mechanics and Rock Engineering, Vol. 49, no. 5 (2016), pp 1679-1693.

Macias, F.J. (2016). Hard Rock Tunnel Boring: Performance predictions and cutter life assessments. PhD thesis, Norwegian University of Science and Technology (NTNU), December, 2016. Trondheim, Norway.

Macias, F.J., Dahl, F. and Bruland, A. (2017). Applicability of the new rock abrasivity test method (RIAT) to cutter life assessments in hard rock tunnel boring. Proceedings of the World Tunnel Congress 2017 – Surface challenges – Underground solutions. Bergen, Norway.

Nærland, J. (2015). Failure mechanisms in cutter tools for tunnel boring. MSc thesis, Norwegian University of Science and Technology (NTNU), Trondheim, Norway (2005).

Roby, J, Sandell, T, Kocab, J and Lindbergh, L (2009). The Current State of Disc Cutter Design and Development Directions. Mining Engineering, Vol. 61, no.3 (2009), pp 36-45

Rostami, J. (1997). Development of a force estimation model for rock fragmentation with disc cutters through theoretical modelling and physical measurement of crushed zone pressure, PhD Thesis. Colorado School of Mines, Golden, Colorado, USA (1997).

Uddeholm "Uddeholm Orvar Supreme" September 2015 (on line)
http://www.uddeholm.com/files/PB_orvar_supreme_english.pdf